Discrimination of remanence-carrying minerals in mixtures, using isothermal remanent magnetisation acquisition curves

D.J. Robertson *, D.E. France

Geography Department, University of Liverpool, Liverpool L69 3BX, UK

(Received 28 October 1992; revision accepted 17 November 1993)

ABSTRACT

It is found that, in general, the isothermal remanent magnetisation (IRM) acquired by natural mineral assemblages closely conforms to a cumulative log gaussian (CLG) function of the magnetising field. The experimentally determined area, mean and standard deviation of the underlying log gaussian function are useful for identifying the type, grain-size and concentration of the magnetic minerals present and for correlating samples containing a common magnetic mineral but derived from different sources. If more than one magnetic mineral is present their IRM acquisition curves combine linearly, and may therefore be resolved by a technique of curve fitting so that the type, grain-size and concentration of each magnetic mineral may be estimated separately, provided that the apparent coercivity spectrum of each phase present approximates to a log gaussian function. Mathematical models of the IRM acquisition process appropriate to single-domain, multi-domain and interacting single-domain grain assemblages have been investigated. It is found that the dispersion parameter (DP) of 0.3 which is usually found experimentally in magnetite assemblages is approximated in the multi-domain model, whereas smaller DP values, corresponding to the value of 0.1 sometimes observed in haematite and goethite, are predicted for single-domain assemblages. Modelling demonstrates that the DP would be affected by grain interactions in an assemblage of single-domain grains, but for magnetite the effect is expected to be minimal unless grains are nearly touching each other.

1. Introduction

Using magnetic techniques (see, e.g. Thompson and Oldfield, 1986) it is possible to detect iron oxide minerals in trace concentrations. The insight so obtained into the types of iron oxide minerals present in natural materials may be used to correlate sedimentary horizons with other horizons or source areas and to assess speculations on the nature of chemical processes accompanying sedimentation in certain environments.

Several iron oxides may be simultaneously present in a natural sample. For example, haematite, goethite and magnetite are common in sedimen-

tary rocks, and more than one phase of titano-magnetite (distinguished by titanium fraction and by grain-size) is commonly found in volcanic rocks. Unfortunately, the magnetic properties of these minerals are generally poorly known nonlinear functions of their grain-size and composition, and in practice it is difficult satisfactorily to 'invert' the magnetic measurements to obtain an inventory of coexisting iron oxide mineral concentrations by type, grain-size and composition. Such an inventory would nevertheless be very useful to the sedimentologist or volcanologist. Jackson et al. (1988) have shown that partial anhysteretic remanent magnetisation (ARM) measurements can resolve coexisting magnetite phases of differing grain-size. Isothermal remanent magnetisation (IRM) is considerably larger than ARM in magnitude and is therefore more sensitive to trace

* Corresponding author at: Department of Physics, University of Zimbabwe, P.O. Box MP167, Harare, Zimbabwe.

concentrations of magnetic minerals. It is therefore appropriate to examine the quantitative information which may be derived from the progressive acquisition of IRM.

2. Experimental technique

In practice, the determination of full IRM acquisition curves is very simple. A weighed quantity of sample is packed tightly into a suitable holder which is itself devoid of magnetisable particles. The sample is then subjected to a progressively increasing unidirectional magnetic field. After each increase in applied field the sample is removed and its magnetisation (i.e. its IRM) is measured using a fluxgate spinner magnetometer. The required magnetic fields are most conveniently obtained in the form of pulses about 1 ms in duration using 'pulse magnetometers' in which energy stored in a bank of capacitors is discharged through a coil surrounding the sample.

3. Results of maghemite, haematite and goethite

Fig. 1 shows typical IRM acquisition curves for samples containing the common iron oxide minerals maghemite, haematite and goethite. It

should be noted that the mineral maghemite would be expected to show almost identical magnetic properties to magnetite, from which it is seldom distinguished. The minerals were obtained as massive hand specimens and were hand-ground to a coarse powder and dispersed within a non-magnetic matrix for measurement. Each sample contained approximately 2 g of the magnetic mineral in question.

A log scale has been used to accommodate the pulse fields, which range over three orders of magnitude. For all of the examples shown in Fig. 1, and indeed for many others, the IRM acquisition curve has a simple sigmoid shape, which can be fitted very well in each of the cases shown in Fig. 1 by a cumulative log gaussian (CLG) function:

$$IRM(B)$$

$$= \frac{M_{ri}}{DP(2\pi)^{1/2}}$$

$$\times \int_{-\infty}^{\infty} \exp\left[\frac{(\log(B) - \log(B_{1/2}))^2}{2(DP)^2}\right] d(\log(B)) \qquad (1)$$

where B is measured in milliteslas and all logs are to base 10. M_{ri} is the inferred saturation IRM, and B is the experimentally measured transient magnetic flux density within the pulse mag-
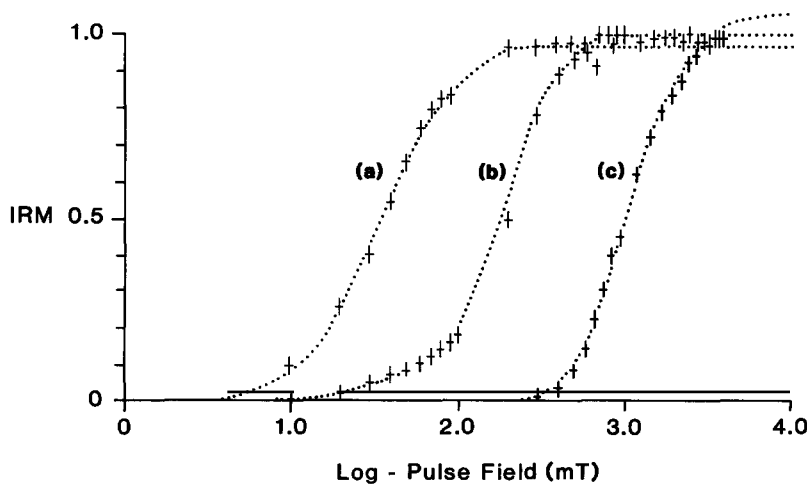
Fig. 1. Experimentally determined IRM acquisition curves for (a) maghemite, (b) haematite and (c) goethite. The constants of normalisation for the y-axis are: (a) 0.908 A m^2 kg^{-1}; (b) 0.322 A m^2 kg^{-1}; (c) 0.090 A m^2 kg^{-1}.

netiser, as calibrated in the absence of any sample. In the following discussion, it will be assumed that the magnetic field intensity (H) experienced by each grain within the sample is B/μ_0; the relative permeability and the demagnetisation field of the bulk sample will be ignored. It will also be assumed that the sample is initially demagnetised.

4. Hypothesis

On the basis of the results shown in Fig. 1, the following hypothesis is advanced: 'The IRM acquisition curve for a single magnetisable mineral phase distributed in a non-magnetic matrix has the form of a cumulative log gaussian function.' This hypothesis is equivalent to postulating that the remanent coercivity spectrum is log-normally distributed for any single magnetisable mineral phase.

The CLG function is described by three parameters:

(1) $B_{1/2}$, the applied magnetic field which causes half of the saturation IRM (SIRM) to be acquired, would be expected to approximate to the coercivity of remanence. It would be distinctive of any particular mineral phase and independent of the concentration of that mineral in a mixture.

(2) The height of the CLG function is the inferred SIRM, or M_{ri}. It would be expected to be equal to the SIRM of the magnetisable mineral phase in question multiplied by its dilution factor in the sample measured.

(3) The dispersion parameter, DP (expressed on a base 10 log scale), reflects the dispersion of apparent coercivities of the domains within the magnetisable mineral phase in question, and would again be expected to be independent of concentration.

5. Superposition of IRM acquisition curves for more than one magnetisable mineral phase

The discussion of $B_{1/2}$, M_{ri} and DP above suggests that it may be possible to infer these parameters (and hence estimate the mineral type, grain-size and concentration) independently for each component in a mixture by fitting a superposition of two or more CLG functions to the experimentally measured IRM acquisition curve. To evaluate this concept, a set of artificial samples was prepared containing mixtures of magnetite and haematite (both prepared by hand-grinding
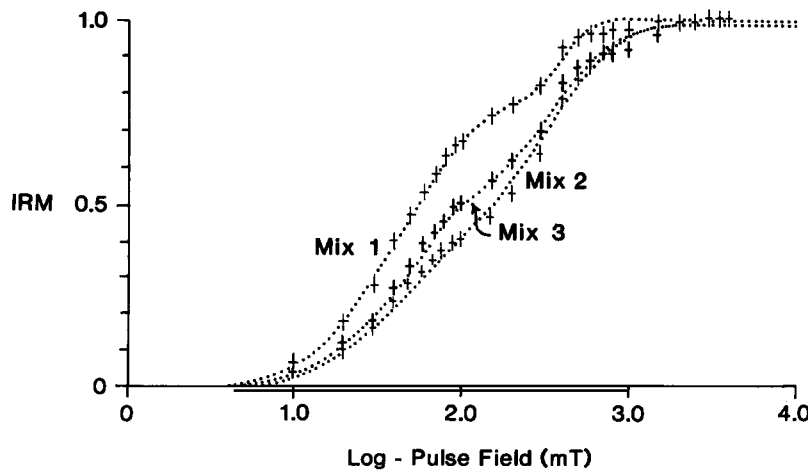
Fig. 2. Normalised IRM acquisition curves for three mixtures containing magnetite, haematite and goethite dispersed in different proportions in a non-magnetic matrix.

hand specimens consisting of massive pure crystals) in various proportions, distributed in a matrix of refractory cement. The role of the cement was to isolate individual magnetic mineral grains and to prevent them from physically rotating in the applied magnetic fields. The complete samples were approximately 10 g in mass and contained the following amounts of added iron oxides:

Mixture 1: magnetite, 0.263 g; haematite, 0.2958 g;

Mixture 2: magnetite, 0.112 g; haematite, 0.5036 g;

Mixture 3: magnetite, 0.222 g; haematite, 0.5032 g;

Mag B2: magnetite, 1.850 g;

AH1: haematite, 4.430 g.

IRM acquisition curves were then measured for each of these samples, and the resulting data points, after subtracting corresponding values for blank samples containing only the refractory cement, are shown as crosses in Fig. 2. Each of these curves clearly shows three inflections, which are attributed to the onset of SIRM in magnetite, haematite and goethite, respectively, from left to right.

The dotted line in the background of Fig. 2 is a two-component CLG function fitted iteratively, by eye, using an interactive computer program. Although the magnetite and haematite curves overlap, the CLG model allows well-determined values to be inferred for the SIRM of each mineral in the mixture. These values are as follows:

Mixture 1: magnetite, 1.122 A m^2 kg^{-1}; haematite, 0.212 A m^2 kg^{-1};

Mixture 2: magnetite, 1.089 A m^2 kg^{-1}; haematite, 0.203 A m^2 kg^{-1};

Mixture 3: magnetite, 0.848 A m^2 kg^{-1}; haematite, 0.200 A m^2 kg^{-1};

Mag B2: magnetite, 0.908 A m^2 kg^{-1};

AH1: magnetite, 0.049 A m^2 kg^{-1}; haematite, 0.274 A m^2 kg^{-1}.

The close similarity in the values so inferred for the SIRM of magnetite in the three mixtures and haematite in the three mixtures shows that for a given magnetisable mineral phase (distinguished by grain-size and grain-shape as well as composition) the value of M_{ri} derived from the IRM acquisition curve is indeed proportional to concentration.

In the case of unmixed samples the iron oxide minerals were present in higher concentrations, of the order of 50% by weight and approximately 10 times their concentrations in the mixtures. Even so, it is difficult to explain why the SIRM for haematite should be higher in the unmixed sample, as grain interactions are not thought to play an important role in this case (see Section 7.3). Perhaps a significant inhomogeneity was encountered in the haematite in the haematite ore, or else the grinding operation resulted in the haematite in specimen AH1 having a different domain state (or grain-size distribution) from that in the mixtures, which were prepared from a second 'batch' of pulverised ore. In the case of Specimen AH1, the pure haematite IRM acquisition curve has moreover developed a 'tail' at low fields which could be confused with the presence of magnetite.

Values for log($B_{1/2}$) and DP for the curves shown in Fig. 2 are as follows:

	Magnetite		Haematite	
	log($B_{1/2}$)	DP	log($B_{1/2}$)	DP
Mixture 1	1.63	0.38	2.54	0.10
Mixture 2	1.65	0.42	2.52	0.18
Mixture 3	1.65	0.36	2.54	0.16
Mag B2	1.55	0.38	–	–
AH1	1.70	0.50	2.30	0.25

This demonstrates that the two iron oxides present are well characterised by very consistent values for $B_{1/2}$ and DP throughout the mixtures, notwithstanding that the concentrations have been varied by factors of two. Log($B_{1/2}$) = 1.65 implies that $B_{1/2}$ and hence B_{cr} is 44.7 mT, and log($B_{1/2}$) = 2.54 implies that $B_{1/2}$ is 347 mT. Again, the effect of very high concentration for the pure samples is evident; for these both $B_{1/2}$ and DP are decreased slightly.

6. Use of IRM acquisition parameters for correlation and provenance determination

From the foregoing, it is evident that the IRM acquisition parameters $B_{1/2}$ and DP can be resolved for individual components of a mixture of iron oxide minerals and are determined by the mineral type and its grain-size, composition and morphology. This raises the possibility of correlating lithologies on the basis of a particular iron oxide mineral phase (e.g. detrital magnetite) in the presence of another (e.g. secondary haematite or fine-grained deuteric magnetite) which is of no stratigraphic significance but would mask simple magnetic characterisation attempts.

A practical example, discussed by Robertson (1993), relates to a deep soil profile (Site PH1) at $37°$ 06.7′ S, $175°$ 01.9′ E in the Hunua Hills, New Zealand. The section comprises a sequence of variously coloured clay horizons on a Mesozoic greywacke substrate in the proximity of Plio-Pleistocene basalt volcanism (Schofield, 1967). Such profiles are common in the district and are attributed to tephra (J.C. Schofield, personal communication, 1992). The description and IRM acquisition signature of the uppermost five layers is shown in Table 1. The values of M_{ri} are large, consistent with relatively high magnetite concentrations as would occur in volcanically derived material. If the SIRM, M_{rs}, for magnetite is taken to be 10 A m² kg⁻¹ (note that M_s is constant but M_{rs}/M_s is a function of grain-size), then M_{ri} = 36.6 mA m² kg⁻¹ implies a magnetite concentration of 0.36 wt.%. Values of M_{ri} vary throughout the section, as is to be expected from the known

tendency for iron oxide minerals to be selectively leached from different parts of the soil profile (see, e.g. Millot, 1970). There is a marked difference between $\log(B_{1/2})$ for the upper layers A–C and for the layers D and E beneath them, which strongly indicates that A–C have a similar provenance and D and E have a similar provenance but there is a distinct difference between the two groups. Thus the profile is interpreted as a sequence of soil zones formed on tephra from two different Plio-Pleistocene volcanic sources; these volcanoes were separated in time by an interval which allowed the formation of a thin soil.

The decision on the number of magnetisable phases present is made on the basis of the number of inflections which can be discerned in the IRM acquisition curve. However, in the case of a suite of volcanic ashes from New Zealand, Robertson (1993) found that a slightly skewed CLG IRM acquisition curve could be elegantly fitted by two superposed CLG functions, each attributable to a distinct phase of magnetite. Moreover, the $B_{1/2}$, DP and M_{ri} values for these two phases corresponded quantitatively to coarse-grained (50 μm) titanomagnetite and fine-grained (1 μm) magnetite. The two phases were positively identified by ancillary studies including physical separations in combination with electron microprobe and thermomagnetic investigations.

Appendix A lists IRM acquisition parameters which have been measured for a variety of natural samples. It is noticeable that DP is generally about 0.3, especially for magnetite. This consistency raises the possibility that DP may be con-

TABLE 1

Layer	Colour (relative)	Thickness (cm)	'Magnetite'			'Haematite'		
			M_{ri} (mA m² kg⁻¹)	$\log(B_{1/2})$	DP	M_{ri} (mA m² kg⁻¹)	$\log(B_{1/2})$	DP
Present soil								
A	Brown	100	12.7	1.47	0.35	–	–	–
B	White	75	36.6	1.47	0.33	–	–	–
C	Orange	25	6.6	1.48	0.36	–	–	–
Thin palaeosoil								
D	Grey	30	4.0	1.35	0.40	1.55	2.7	1.0
E	Orange	100	4.4	1.34	0.36	0.23	3.0	1.0

trolled by the physics of IRM acquisition. Conversely, if DP is determined by dispersion in grain-size, shape and composition of iron oxide crystals then it may be a valuable parameter for cross-correlating natural samples. We now investigate some simple models of IRM acquisition in common classes of naturally occurring magnetisable minerals, to assess the physical significance of DP.

7. Physical models for the IRM acquisition curve

Although the shape of the hysteresis loop for magnetic materials has been much studied (see, e.g. Jiles and Atherton, 1986), the shape of the IRM acquisition curve has received little theoretical attention. In an effort to gain some insight into the significance of the above-mentioned IRM acquisition parameters, it is appropriate to consider the acquisition of remanence for three regimes which can be investigated theoretically, namely: (1) a randomly oriented assemblage of single-domain particles, (2) an assemblage of multi-domain particles and (3) an array of interacting particles.

7.1. Single-domain particles

The following model for IRM acquisition in single-domain grains is essentially equivalent to that incorporated in the study by Stephenson (1983), and produces a similar result. Let us consider a uniaxial single-domain particle with fixed switching field given by $B_{sw} = 2K_u/(M_s)$, where K_u is the magnetocrystalline anisotropy and M_s is the spontaneous magnetisation. Then, according to the model of Stoner and Wohlfarth (1948) (based on uniformly magnetised prolate ellipsoidal grains), the field required to flip the magnetisation vector when the easy axis of magnetisation is aligned at an angle θ to the field is

$$B = \frac{2K_u(1 - w^2 + w^4)^{1/2}}{M_s(1 + w^2)} \qquad (2)$$

where

$$w = (\tan \theta)^{1/3}.$$

Now for a randomly oriented assemblage of single-domain grains the fraction of grains which
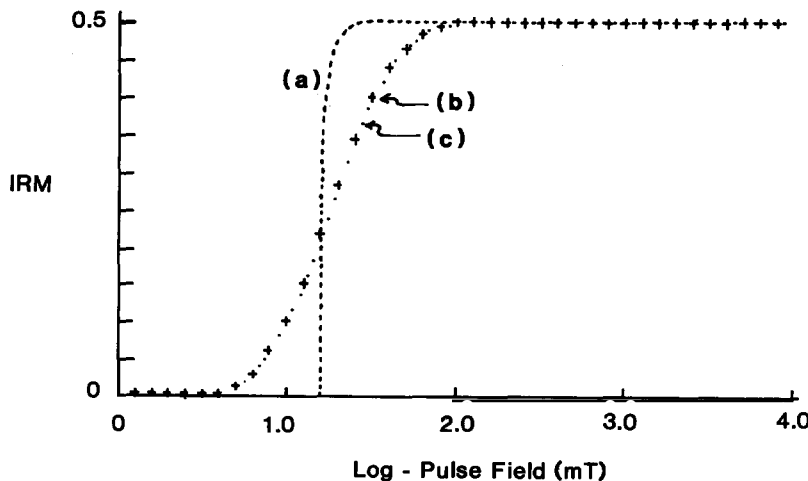
Fig. 3. (a) Theoretical IRM acquisition curve for an assemblage of randomly oriented non-interacting single-domain uniaxial grains. (b) The effect of convoluting Curve (a) with a log normal function. (c) A CLG function fitted to Curve (b).

have their easy axes aligned within the annular cone $\theta + d\theta$ to θ will be

$\mathrm{Pr}(\theta < \text{alignment angle} < \theta + d\theta)$

$$= \frac{R \, d\theta \cdot 2\pi R \sin \theta}{4\pi R^2}$$

$$= \tfrac{1}{2}\sin \theta \, d\theta \qquad (3)$$

The contribution of such a grain to the final IRM will be the vector component of its dipole moment in the direction of the applied field, and hence the expected value of IRM will be

$$\hat{M}(B) = M_s \int_0^{\pi} \frac{Q(\theta, B) \cos \theta \sin \theta \, d\theta}{2} \qquad (4)$$

where $Q = 1$ if the applied field is greater than $B_{sw} \cdot (1 - w^2 + w^4)^{1/2}/(1 + w^2)$ and $Q = 0$ otherwise.

Eq. (4) has been evaluated numerically, and the resulting IRM acquisition curve is shown as Curve (a) in Fig. 3. The figure is scaled such that $2K_u/M_s$ is 31.6 mT, a reasonable value for magnetite. For ready comparison, the scales used in Fig. 3 have the same meanings as those used in Figs. 1 and 2. The IRM acquisition curve for the randomly oriented single-domain grains rises very abruptly and becomes rounded as it acquires its final value. The curve may be approximated very roughly by a CLG function (not shown) with $B_{1/2} = 17.8$ mT. If the particles were not exactly uniform, but had variable shape and composition, then the IRM acquisition curve would become rounded. This concept was explored by Gaunt (1960), using a rectangular distribution function for anisotropy fields to explain the sigmoid shape of DC demagnetisation curves. If B_{sw} was log-normally distributed, then the IRM acquisition curve would be the convolution product of this log-normal curve with Curve (a) in Fig. 3. Not surprisingly, the resulting IRM acquisition curve, which is shown as curve (b) in Fig. 3, can be closely fitted by a CLG function. In the case of this curve, the mean switching field was chosen to be 31.6 mT (log $B_{sw} = 1.5$) and the standard deviation of the gaussian distribution function was 0.3 (on the scale of $\log_{10}$). The fitted CLG function, Curve (c) in Fig. 3, has $B_{1/2} = 18.2$ mT (log $B_{1/2} = 1.26$) and DP = 0.3. Thus if the single-domain

model is applicable to real magnetic mineral assemblages then $B_{1/2}$ is likely to be about half the mean value of the switching fields $(2K_u/M_s)$ for the grains present and DP is likely to be dominated by the distribution of switching fields among the grains rather than by the effects of random grain orientation.
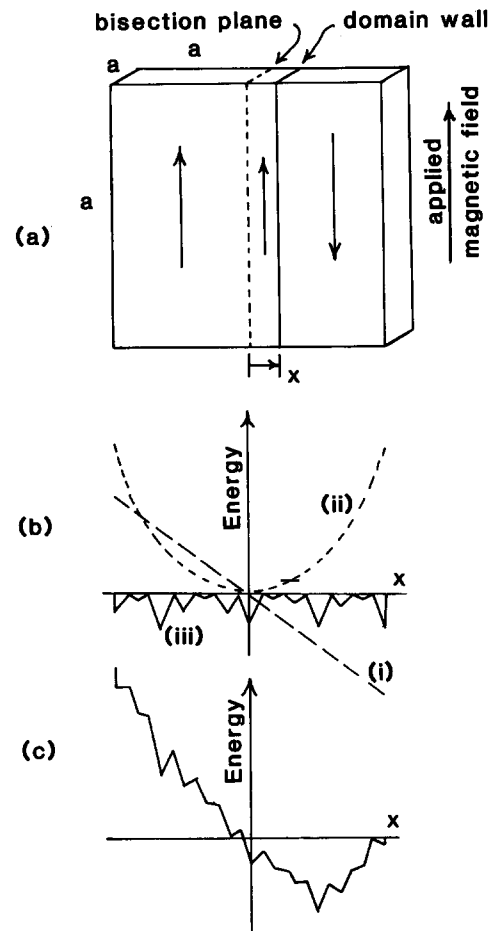
Fig. 4. Two-domain cubic uniaxial grain model. (a) Domain magnetisation directions in the presence of an external magnetic field. (b) Form of: (i) energy related to external magnetic field; (ii) self energy; (iii) energy related to modelled equally spaced pinning sites of random depth. (c) Total magnetic energy as a function of domain wall displacement x for a particular applied magnetic field. A stronger upward field would force the minimum to the right.

7.2. Multi-domain grains

To a first approximation, the acquisition of IRM by multi-domain grains may be modelled by a two-domain cubic grain (Fig. 4(a)) having a Bloch wall parallel to a pair of faces and to the applied field. If x is the displacement of the wall from the centre of the grain then the magnetisation energy of the grain is a linear function of x for any particular applied field (the product of the total dipole moment and the applied field), superimposed on an approximately quadratic function of x related to the interaction of the oppositely magnetised domains with each other and the self-demagnetisation energy within each domain (Fig. 4(b)). In the numerical model the energy of interaction within and between the two domains was modelled using the exact expression of Rhodes and Rowlands (1954) (Appendix A).

For any given applied field the domain wall would move to an energy minimum and thereby enlarge the domain magnetised in the field direction. However, on removal of the field the wall would return to the central position. IRM (and hysteresis) is only possible if the domain wall is prevented from returning to the central position by 'pinning sites' where crystal defects cause local

energy minima to trap the domain wall as it moves across the grain (Fig. 4(c)). For the two-domain grain, pinning sites have been modelled by 100 regularly spaced triangular traps. This model was inspired by that of O'Reilly (1984, p. 79), whereby defects were modelled by a sinusoidal perturbation energy profile across the grain. The domain wall becomes pinned if the energy gradient at one side of a trap overcomes the energy gradient at that location caused by the self-demagnetisation and the applied field. Each of the 100 barriers has been modelled with an edge gradient taking a random value between zero and an arbitrarily allocated threshold.

With this model, the process of pulse magnetisation and IRM acquisition can be replicated in a computer. For a given applied field the wall moves in the direction of lowest total energy until it is blocked by an edge with contrary energy gradient. The field is then removed and the wall moves back toward the centre of the grain until it is again blocked by a contrary energy gradient. The displacement of the domain wall at this point is proportional to the IRM.

If the plane of the domain wall is oblique to the easy magnetisation axis of the domains, the energy due to the applied field will be a vector
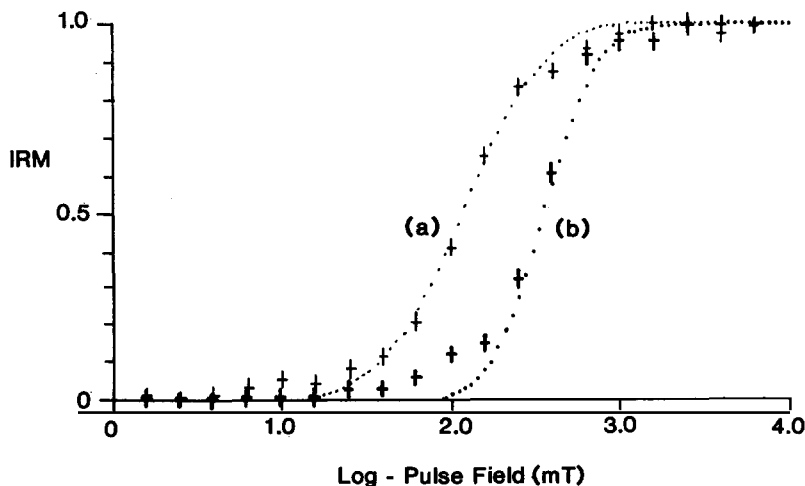
Fig. 5. Modelled IRM acquisition curves for an assemblage of randomly oriented uiniaxial two-domain cubic grains. For Curve (b) the maximum energy depth of the random defects is 2.5 times greater than for curve (a) and the M_{rs}/M_s ratio (which is the y-axis normalisation factor) has increased from 0.15 to 0.51. Crosses are points computed according to the model and the dotted lines are fitted CLG curves discussed in the text.

dot product. Moreover, for an assemblage of randomly oriented grains the contribution of the grain to the overall magnetisation of the assemblage may be taken to be its component of magnetisation in the direction of the applied field. Thus the IRM acquisition curve for an assemblage of randomly oriented uniaxial two-domain grains can be modelled by selecting a random orientation angle (i.e. a difference angle between the orientation of the easy axis and the applied field, with appropriately weighted probability) and applying the algorithm described above.

The model has been implemented in BASIC using a personal computer. The program works by first setting up a table of reduced self energies for each of 100 equally spaced possible domain wall positions from one edge of the cubic grain to the other. A grain is then selected by nominating its attitude angle relative to the applied field using a data table of 10 equally likely angle intervals from which one is chosen at random. The domain wall is then stepped across the grain until it encounters a pinning site whose energy gradient is upward in the presence of the applied field. Because, in this model, the wall will remain in the same position after the field is removed, the IRM can then be calculated. To replicate the effect of a large number of randomly oriented grains, this process has been applied iteratively to 1000 grains for each applied field step.

The results are shown in Fig. 5. Scaling follows from adopting $M_s = 4.8 \times 10^5$ A m^{-1} (corresponding to magnetite), and is independent of the size of the cubic grain. The scale factor (SF) for the maximum slope of the random barriers is effectively arbitrary. In Fig. 5(a), SF is 0.2, and it can be seen that a sigmoid IRM acquisition curve results, corresponding to a CLG curve with $\log(B_{1/2}) = 2.07$ or $B_{1/2} = 117$ mT, and the normalisation constant used for the ordinate implies an M_{rs}/M_s ratio of 0.15. For Fig. 5(b), SF has been set at 0.5 so that the depth of the energy minima at the pinning sites has increased 2.5-fold. The consequence of this is (not surprisingly) that the assemblage is more difficult to magnetise, as $\log(B_{1/2})$ increases to 2.55 ($B_{1/2} = 350$ mT), and is magnetically harder because, from the constant of normalisation used for the ordinate, an M_{rs}/M_s

ratio of 0.51 is implied. The values of the fitted DP parameter in Figs. 5(a) and 5(b), respectively, are 0.38 and 0.25, which are to be compared with values of 0.3–0.4 associated with natural magnetite assemblages discussed in this paper.

The fit to a CLG function appears to be good, although there is in each case a small offset, about 10% of the total M_{ri}, at the left end of the curve. Such an offset detracts from the elegance of the CLG hypothesis, but a 'tail' to the left of an experimentally determined IRM acquisition curve was noted in Section 5 for haematite at such high concentrations that interacting grains could behave like multi-domain grains. Incidentally, the CLG shape obtained in the model curves is not generated by the randomness of the grain orientations. IRM acquisition curves of almost identical shape but having $\log(B_{1/2})$ reduced by 0.15 were obtained if the grains were all aligned with the applied field.

7.3. The effect of interacting grains

The general features of remanence acquisition in assemblages of interacting single-domain grains were discussed by Kneller (1968). His analysis is in terms of mathematically tractable, but somewhat artificial, models for grain orientation and does not, in fact, yield IRM curves against which the CLG hypothesis can be closely tested.

Fearon et al. (1990) have presented a computer model to investigate the effect of grain interactions, involving a geometrical array of uniaxial single-domain grains, with gaussian-distributed size and switching field. A smooth sigmoid IRM acquisition curve was obtained. Notwithstanding this agreement with observation, the model of Fearon et al. (1990) does not predict the circumstances under which interaction effects would become significant in a natural assemblage. Indeed, it is not clear whether the sigmoid shape of their IRM acquisition curve is due to interaction at all, as the chosen distribution of switching fields could have the same effect.

To complement the model of Fearon et al. (1990), an alternative numerical model has been implemented on a personal computer (using Pascal). The model comprises a regular $10 \times 10 \times 10$

cubic array of spherical uniaxial single-domain crystals of equal size. A random orientation in three dimensions is allocated to each crystal and this orientation is thereafter not changed. The polarity of magnetisation is described as positive if it lies in the forward hemisphere relative to the axis along which a magnetic field will subsequently be applied, and is negative otherwise. The magnetisation polarity of each crystal is allocated randomly at the outset.

The dipole field of each such grain is then calculated for the site of nearby grains. In doing this, the dipole is resolved into three orthogonal components and field produced at the 'end-on' and 'broadside' sites relative to each component are calculated out to two lattice spacings, whereas otherwise only adjacent sites are considered. Thus for each orthogonal component of the dipole moment of each grain the three-dimensional field produced is calculated for 32 nearby sites. Where the nearby sites would lie beyond the edges of the defined matrix, the calculated parameters are applied to sites on the opposite side of the matrix as if it were a unit cell of a system of identical structures extending indefinitely in every direction.

A magnitude is then chosen for the applied magnetic field. The magnetic field present at the site of each crystal in turn is next computed from the vector sum of the external field and the already calculated dipole fields related to nearby grains. If the vector dot product of this magnetic field and a unit vector in the direction of the crystal axis is negative and exceeds a predetermined 'switching field', then the magnetic polarity of the grain is reversed. This simplified switching criterion is justified by the sharpness of the onset of magnetisation for randomly oriented single-domain grains (deduced in Section 7.1 above) and the pragmatic requirement for a switching criterion which is economical in terms of machine computation time. Each successive grain is considered in turn, and switching is carried out before moving on to the next grain. Thus it is necessary to pass repeatedly through the matrix until a stable situation is attained when no further switching is indicated. In practice, the algorithm converges rapidly to a stable result, normally within six passes.

After magnetising the array in the presence of an applied field, the IRM is found by repeating the whole process with the applied field set to zero. In practice, the second step did not alter the solution, which means that the M_{rs}/M_s ratio for this model is unity.

Integer arithmetic is used to optimise memory
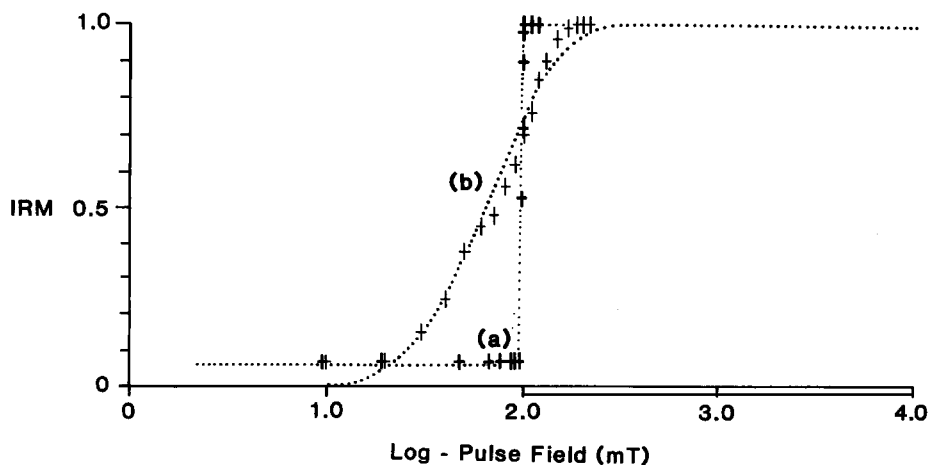
Fig. 6. IRM acquisition curves for a regular array of randomly oriented uniaxial single-domain grains which are able to interact. The switching field for each grain is 100 mT. Grain diameter 30 μm. In Curve (a), grain spacing is 200 μm; in Curve (b), grain spacing is 30 μm.

and processing time. In doing so, the magnetic fields are scaled in terms of the parameter

$$Q = \frac{\mu_0 M_s (\text{grain diameter})^3}{3 (\text{lattice spacing})^3}$$ (5)

which has the units of tesla and is compared with the switching field (B_{sw}) after the applied field (B_{ext}) has been added. Thus it is the ratio of grain diameter to lattice spacing and the ratio of saturation magnetisation (M_s) to switching field which determine the shape and position of the IRM acquisition curve.

IRM acquisition curves computed using this model with physical parameters associated with magnetite, namely $B_{sw} = 100$ mT and $M_s = 4.8 \times 10^5$ A m^{-1}, are shown in Fig. 6. It can be seen that the onset of magnetisation for the assemblage is very sharp unless the lattice spacing is so small that the grains are almost touching, in which case the IRM acquisition curve is rounded to a form which can be approximated by the cumulative log gaussian function. It is also noticeable that the effect of interactions is to reduce $B_{1/2}$ to a value which is less than the switching field for individual grains.

If the switching field for magnetite were 50 mT then the curve of Fig. 6(b) would correspond to a grain spacing of 240 μm. For haematite, B_{sw} is greater (by an order of magnitude) and M_s is much less (by about three orders of magnitude), so interaction between haematite grains will scarcely affect the IRM acquisition curve even if the grains are touching each other. Similarly, interaction between goethite grains would not be expected to influence the IRM acquisition curve.

8. Conclusions

It is concluded that the IRM acquisition curve of naturally occurring distributions of iron oxide minerals can, in general, be reasonably well fitted by a linear combination of cumulative log gaussian functions, each corresponding to a single magnetisable mineral phase. From the fit, it is possible, within broad bounds, to estimate the type, grain-size and concentration of the mineral

phases in question. Computer models of the IRM acquisition process suggest that the onset of IRM should be abrupt in an assemblage of single-domain grains of uniform size, and in the case of multi-domain magnetite a dispersion parameter (DP) of approximately 0.3 would be expected, as is in fact observed. A rounding of the IRM acquisition curves would also be expected to arise from grain interactions, but the models indicate that such interactions would become significant only when the separation of the magnetisable grains approaches their own diameters.

References

Dunlop, D.J., 1983. On the demagnetising energy and demagnetising factor of a multidomain ferromagnetic cube. Geophys. Res. Lett., 10: 79–82.

Fearon, M., Chantrell, R.W. and Wohlfarth, E.P., 1990. A theoretical study of interaction effects on the remanence curves of particulate dispersions. J. Magnetism Magnetic Mater., 86: 197–206.

Gaunt, P., 1960. A magnetic study of precipitation in a gold–cobalt alloy. Philos. Mag., 5: 1127–1145.

Jackson, M., Gruber, W., Marvin, J. and Banerjee, S.K., 1988. Partial anhysteretic remanence and its anisotropy: applications and grain-size dependence. Geophys. Res. Lett., 15: 440–443.

Jiles, D.C. and Atherton, D.L., 1986. Theory of magnetic hysteresis. J. Magn. Magn. Mater., 61: 48–60.

Kneller, E., 1968. Magnetic interaction effects in fine particle assemblies and in thin films. J. Appl. Phys., 39: 945–955.

Millot, G., 1970. Geology of Clays. Chapman and Hall, London, 429 pp.

O'Reilly, W., 1984. Rock and Mineral Magnetism. Blackie, Glasgow, 220 pp.

Rhodes, P. and Rowlands, G., 1954. Demagnetising energies of uniformly magnetised rectangular blocks. Proc. Leeds Philos. Lit. Soc., Sci. Sect., 6: 191–210.

Robertson, D.J., 1993. Discrimination of tephra using rock-magnetic characteristics. J. Geomagn. Geoelectr., 45: 167–178.

Schofield, J.C., 1967. Geological Map of New Zealand, 1:250000, Sheet 3, Auckland. NZ Geological Survey, Department of Scientific and Industrial Research, Wellington, New Zealand.

Stephenson, A., 1983. Changes in direction of the remanence of rocks produced by stationary alternating field demagnetisation. Geophys. J. R. Astron. Soc., 73: 213–239.

Stoner, E.C. and Wohlfarth, E.P., 1948. A mechanism of magnetic hysteresis in heterogeneous alloys. Philos. Trans. R. Soc. London, Ser. A, 240: 599–624.

Thompson, R. and Oldfield, F., 1986. Environmental Magnetism. Allen and Unwin, London, 227 pp.

Appendix A

From Dunlop (1983), based on Rhodes and Rowlands (1954), the self energy density of two domains shown in Fig. 4(a) (i.e. the sum of the self energy for each domain and the interaction energy for the pair) can be shown to be

$$E = 2\mu_0 M_s^2 \left[2\Delta F\left(\tfrac{1}{2} + x/a, 1\right) + 2\Delta F\left(\tfrac{1}{2} - x/a, 1\right) - \Delta F(1, 1) - \Delta F(0, 1) \right]$$

where $\Delta F(p, q) = F(p, 0) - F(p, q)$ and F is the Rhodes and Rowlands (1954) function:

$$
\begin{aligned}
F(p, q) = {} & \left(p^2 - q^2\right) \sinh^{-1}\left(p^2 + q^2\right)^{-1/2} \\
& + p\left(1 - q^2\right) \sinh^{-1}\left[p\left(1 + q^2\right)^{-1/2}\right] \\
& + pq^2 \sinh^{-1}(p/q) - \pi pq \\
& + q^2 \sinh^{-1}(1/q) \\
& + 2pq \tan^{-1}\left[q\left(1 + p^2 + q^2\right)^{1/2}/p\right] \\
& - \left(1 + p^2 - 2q^2\right)\left(1 + p^2 + q^2\right)^{1/2}/3 \\
& + \left(1 - 2q^2\right)\left(1 + q^2\right)^{1/2}/3 \\
& + \left(p^2 - 2q^2\right)\left(p^2 + q^2\right)^{1/2}/3 + 2q^3/3
\end{aligned}
$$

Appendix B: IRM acquisition parameters for some natural materials

Sample [a]	Magnetite [b]		Haematite [b]		Goethite [c]		Reference
	Log($B_{1/2}$)	DP	Log($B_{1/2}$)	DP	Log($B_{1/2}$)	DP	
1. Loess	–	–	1.85	0.35	3.5	1.0	a
2. Basalt	1.45	0.35	–	–	–	–	b
3. Tephra	1.47	0.35	–	–	–	–	c
4. Fly ash	1.60	0.31	–	–	3.5	1.0	d
5. Furnace exhaust	–	–	1.72	0.32	3.0	1.0	d
6. Roman pottery	–	–	1.91	0.26	–	–	e
7. Goethite (A1G1)	–	–	–	–	3.4	0.30	b
8. Goethite (A2G1)	–	–	–	–	3.1	0.27	b
9. Goethite (A3G1)	–	–	–	–	3.4	0.21	b
10. Goethite (A4G)	–	–	–	–	2.8	0.50	b
11. Haematite (AH1)	–	–	1.70	0.50	2.3	0.25	b
12. Haematite (AH2)	–	–	1.62	0.25	3.0	0.35	b
13. Haematite (AH3)	–	–	1.85	0.40	3.0	0.10	b
14. Haematite (AH4)	–	–	1.35	0.32	2.3	0.25	b
15. Haematite (AH5)	–	–	1.70	0.50	2.3	0.25	b

Sources: (a) T.C. Rolph, personal communication, 1988; (b) this study; (c) Robertson (1983); (d) E. Salinovic, personal communication, 1988; (e) D. Atkinson, personal communication, 1991.

[a] All samples were naturally occurring. Samples 7–15 were ores.

[b] In Samples 4, 5 and 11–14 there is ambiguity in the identification of an inferred magnetic phase on the basis of IRM acquisition data alone because the remanent coercivity spectra of magnetite and haematite overlap (O'Reilly, 1984, pp. 145, 146 and 185).

[c] Goethite is not saturated by the available pulse field of 3 T. Therefore log ($B_{1/2}$) and DP are poorly determined for this mineral.